Published in final edited form as:
Dev Dyn. 2009 February ; 238(2): 358–366. doi:10.1002/dvdy.21681.

Fgf16^{IRESCre} mice: A tool to inactivate genes expressed in inner ear cristae and spiral prominence epithelium

Ekaterina P. Hatch[1], **Lisa D. Urness**, and **Suzanne L. Mansour**
Department of Human Genetics, University of Utah, Salt Lake City, UT 84112-5330

Abstract

Fibroblast growth factors play important roles in inner ear development. Previous studies showed that mouse *Fgf16* is expressed asymmetrically during the otic cup and vesicle stages of development, suggesting roles in regulating or responding to anteroposterior axial cues. Here, we studied otic *Fgf16* expression throughout embryonic development and found transcripts in the developing cristae and in a few cells in the lateral wall of the cochlear duct. To determine the otic function of *Fgf16* and to follow the fate of *Fgf16*-expressing cells, we generated an *Fgf16*^{IRESCre} allele. We show that *Fgf16* does not have a unique role in inner ear development and that the *Fgf16* lineage is found throughout the three cristae, in portions of the semicircular canal ducts, and in the cochlear spiral prominence epithelial cells. This strain will be useful for gene ablations in these tissues.

Keywords

Fibroblast growth factor; mouse mutant; lineage; semicircular canals; vestibular system; cochlear duct; spiral prominence; otic cup and vesicle; embryo

Introduction

The inner ear is a morphologically complex organ specialized for sensing sound and relative head motion. In the mouse, epithelial mechanosensory patches are found in six locations. Sound-responsive cells are located along the length of the coiled and ventrally located cochlear duct. The remaining motion-responsive sensory patches are housed within the dorsally located vestibular system. Two sensory organs, the maculae of the utricle and saccule respond to changes in linear motion and three additional sensory organs, the anterior, lateral and posterior cristae, each one located at the base of a semicircular canal, respond to changes in angular motion.

Remarkably, the entire inner ear epithelium is derived from a patch of head ectoderm that is morphologically evident as a placodal thickening at embryonic day (E)8.0 in the mouse (~8–9 somites). Subsequently, from E8.5–E9.0 (~13–20 somites), the placode invaginates to form the otic cup, which continues to deepen, and by E9.5 (~25 somites) closes and separates from the surface ectoderm, forming the roughly spherical otic vesicle. Morphogenesis of the vesicle initiates at E10–10.5 with a dorsomedially directed outgrowth of the endolymphatic duct/sac (EDS) anlage and a ventrally directed outgrowth of the cochlear duct. During the next few days of development, this relatively simple epithelium acquires its mature and complex morphology and begins to differentiate its six sensory

Corresponding Author: Suzanne L. Mansour, Department of Human Genetics, University of Utah, 15 North 2030 East, Rm. 2100, Salt Lake City, UT 84112-5330, Phone: 801-585-6893, Fax: 801-581-7796, e-mail: suzi.mansour@genetics.utah.edu.
[1]Current address: Department of Anatomy and Neurobiology, Washington University School of Medicine, St. Louis, Missouri 63110

patches. Morphogenesis is essentially complete by E15.5, but sensory differentiation continues even through the early postnatal period (Swanson et al., 1990; Morsli et al., 1998; Kiernan et al., 2002).

The ear is an asymmetric structure with each of its developmental axes having distinct morphologic characteristics. For example, the anterior and lateral cristae are anterior structures and the posterior crista is a posterior structure. Although much remains to be determined regarding the timing and order of otic axis initiation and fixation, particularly in the mouse (Bok et al., 2007), it is clear that patterns of gene expression in the otic placode tend to be relatively uniform, and cell fates, as assayed in the chick, are not compartmentalized at this stage (Streit, 2002). Asymmetric otic gene expression can first be discerned at the otic cup stage, when the anteroposterior (AP) axis (likely the first axis to be fixed) is starting to be established (Wu et al., 1998), and fate maps generated by marking chick otic cup cells at stage 13.5 (~20–21 somites) suggest that a compartment boundary separating anterior and posterior cell fates has already formed (Brigande et al., 2000).

We showed previously that *Fgf16* transcripts are regionally restricted and polarized along the AP axis of the otic cup and vesicle. *Fgf16* expression initiated at the early otic cup stage (13 somites) and was concentrated in a posterior spot. By the early otic vesicle stage (24 somites), *Fgf16* was found in a posterodorsolateral spot (Wright et al., 2003). These observations suggested possible signaling roles for FGF16 in otic axis formation and/or cell fate decisions. In addition, the seemingly transient posterior expression of *Fgf16* pointed to the opportunity to map the fate of these cells and compare the results with fate maps established by cell marking techniques in other species. To this end, we studied the *Fgf16* otic expression pattern throughout embryonic development and generated a targeted mutant mouse strain in which *Fgf16* expression was ablated and CRE recombinase was expressed in its place. We found that *Fgf16* transcripts continue to be expressed beyond the early otic vesicle stage and mark all three developing cristae. We also detected cochlear duct expression of *Fgf16* that was confined to a few cells in the lateral wall. Mice bearing an *IRESCre* insertion disrupting *Fgf16* expression did not exhibit any structural or functional otic abnormalities, but lineage studies of the $Fgf16^{IRESCre}$ strain revealed that all three cristae, but not the maculae or cochlear sensory tissue, are derived from the early posterior, and a subsequent anterior patch of *Fgf16*-expressing cells, and that derivatives of these cells also populate a proportion of the non-sensory semicircular canal ducts, prior to any expression of *Fgf16* in the ducts. The *Fgf16* lineage in the cochlear duct marked precursors of spiral prominence epithelial cells, which may contribute to the regulation of endolymph composition (Slepecky, 1996; Santi and Tsuprun, 2001), and thus auditory function. Our results suggest that the $Fgf16^{IRESCre}$ strain may be a useful tool in conditional ablation experiments designed to isolate the function of genes expressed in the developing cristae and/or spiral prominence epithelial cells from their functions in other inner ear tissues.

Results and Discussion

Fgf16 is initially expressed asymmetrically in the otic cup and vesicle, and subsequently in all three semicircular canal cristae and in the lateral wall of the cochlear duct

Previous studies showed that both mouse and chick *Fgf16* expression is regionally restricted during the early phases of inner ear development (Wright et al., 2003; Chapman et al., 2006). To obtain a more detailed picture of mouse otic *Fgf16* expression, we studied closely staged embryos throughout development (Fig. 1). Otic expression of *Fgf16* was first detected weakly in the posterior otic cup of 14-somite embryos (E9.0, Figs. 1A,A′). By 17 somites (E9.0), as the cup started to close to form the otic vesicle, *Fgf16* transcripts were more strongly expressed and still localized to the posterior cup (Figs. 1B,B′). Starting at 21 somites (E9.5), when the vesicle formed (data not shown) and subsequently at 23 somites

(E9.5), *Fgf16* was detected in the posterior otic vesicle, marking the dorsolateral region (Figs. 1C,C′). By 28–30 somites (E10.0), *Fgf16* expression was further restricted to a posterolateral domain, located midway between the dorsal and ventral poles of the vesicle (Figs. 1D,D′,E,E′). Finally, at 40 somites (E11.0), *Fgf16* as found in two spots in the developing cristae (Fig. 1F; a/lc, anterior/lateral cristae; pc posterior crista). Extra-otic sites of embryonic *Fgf16* expression at these stages included the developing posterior pharyngeal pouch endoderm and olfactory placode/epithelium (supplementary Figs. S1A-D″), however, unlike in zebrafish embryos (Nomura et al., 2006), mouse *Fgf16* expression was not detected in the limb apical ectodermal ridge (data not shown).

To determine whether *Fgf16* expression persisted in the otic region later in development, we detected *Fgf16* transcripts at E11.5, E13.5, E14.5 and E16.5 in transverse sections and at E18.5 in sagittal sections taken through the head. At E11.5, *Fgf16* expression was found in all three developing cristae, but not in other regions of the developing semicircular canal ducts (Figs. 1G,H; ac, anterior crista; lc, lateral crista; pc, posterior crista). In addition, several cells at the lateral (non-sensory) edge of the cochlear duct (cd) expressed *Fgf16* (Figs. 1I–K, arrow). Expression was stronger at the apex (Fig. IK) than at the base of the duct (Fig. 1I). At E13.5, *Fgf16* transcripts continued to be expressed in the developing cristae (Figs. 1L,L′,N), and weak expression extended into adjacent patches of presumptive non-sensory epithelium of the semicircular canals (see for example the anterior semicircular canal in Fig. 1L′), but was completely absent from the developing saccular and utricular sensory patches (Fig. 1M). In addition, *Fgf16* continued to be expressed in a few cells of the lateral wall of the cochlear duct (Fig. 1N,N′, arrows). At E14.5, *Fgf16* expression in the cristae persisted, but began to weaken (Figs. 1O,O′,P). A discrete patch of expression in the thin canal wall opposite the cristae was also apparent (Figs. 1O,O′; arrow in O′). This expression in non-sensory canal tissue extended a short distance away from the cristae. *Fgf16* expression in the lateral cochlear duct continued through E14.5 (Figs. 1Q,Q′). Although *Fgf16* could still be detected weakly in the cristae at E16.5 and E18.5 (Figs. 1R,R′,S), its expression was markedly reduced relative to earlier stages. In contrast, expression in the lateral cochlear duct remained strong (Figs. 1R,R″,T). Extra-otic sites of *Fgf16* expression detected in this series of sections through a portion of the head included the anterior pituitary and olfactory epithelium (supplementary Figs. S1E-F′).

These results show that *Fgf16* expression in the mouse inner ear persists beyond the stages originally analyzed (Wright et al., 2003). As in the chick embryo (Chapman et al., 2006), mouse *Fgf16* is expressed initially in a pattern similar to that of *Bmp4*, a gene that marks the developing cristae and is required for their development and that of their associated semicircular canals (Morsli et al., 1998; Chang et al., 2008). Zebrafish *Fgf16* is also expressed in the otic vesicle, but whether it is regionalized is unknown (Nomura et al., 2006). The early asymmetric expression of *Fgf16* in the posterior and then posterolateral regions of the mouse otic vesicle suggests possible roles in or responses to signaling for otic axis formation or cell type specification, particularly in the prospective vestibular system. The subsequent restriction of *Fgf16* expression to the developing cristae suggests roles in distinguishing this type of sensory development from that of the maculae. It is interesting to note that unlike *Bmp4*, which ultimately marks the supporting cells of the cristae (Morsli et al., 1998), *Fgf16* expression in the cristae does not resolve to distinguish the sensory vs. supporting cell populations, but rather is strongly reduced by E16.5 as this distinction develops.

Expression of *Fgf16* in the developing cochlear duct starting at E11.5 is remarkably restricted and persistent in a few cells that appear to lie at the base of the developing stria vascularis, which is required for generation and maintenance of the endocochlear potential needed for hearing function. Although *Bmp4* is also expressed from E11.5 in the developing

cochlear duct, its domain is likely non-overlapping with that of *Fgf16* in this tissue, as *Bmp4* marks the precursors of Hensen and Claudius cells (Morsli et al., 1998); whereas *Fgf16* marks more laterally located cells. The functional significance of these particular *Fgf16*-expressing cells, however, is unknown.

Gene targeting at the Fgf16 locus

To observe the consequences of *Fgf16* inactivation and to follow the fate of *Fgf16*-expressing cells originating in the posterior otic epithelium and later in the cochlear duct, we targeted the *Fgf16* locus using a vector containing an internal ribosomal entry site (IRES) preceding a *Cre* gene, which was followed by an frt-flanked *Neo* selection cassette (Fig. 2A) (Arenkiel et al., 2003). To generate a null allele, the *IRES-Cre-Neo* cassette was placed in the first coding exon of *Fgf16* (Fig. 2A), preventing production of the majority of the protein, in particular, the predicted FGFR-binding sequences located between two conserved cysteines.

The insertion mutation was introduced into X-linked *Fgf16* in male ES cells through standard gene targeting protocols. Correctly targeted cell clones, hemizygous for the introduced mutation, were identified by Southern blot hybridization analysis of *Tth111I*-digested DNA using a 5′ flanking external probe and of *HindIII*-digested DNA using a 3′ internal probe, which caused the predicted shifts of wild type *Fgf16* DNA from 8.4 kb to 10.5 kb and 18 kb and 14.8 kb, respectively (Figs. 2A,B). Mice bearing the targeted allele, $Fgf16^{IRESCreNeo}$ (MGI accession number 3790778, symbolized $Fgf16^{tm1(Cre)Sms}$), were generated by standard procedures.

To determine the efficacy of the disruption strategy, an RT-RCR reaction was performed to detect *Fgf16* mRNA in wild type and mutant animals (Figs. 2A,C). Using primers that flank the IRES-*Cre-Neo* insertion site (Fig. 2B), the expected DNA fragment of 281 bp was evident in wild type and heterozygous female samples, but was absent from a male hemizygous mutant sample. In contrast, all samples expressed the X-linked *Hprt* gene, showing that the targeting strategy specifically disrupted production of normal *Fgf16* mRNA.

Fgf16 is not required for mouse development

To determine whether *Fgf16* is required for any aspect of embryonic or postnatal development, the F1 female $Fgf16^{IRESCreNeo/+}$ offspring of germline chimeras were mated to wild type males or F2 $Fgf16^{IRESCreNeo/Y}$ males, and adult progeny were genotyped. The numbers of each genotype were consistent with a normal Mendelian distribution of wild type and mutant alleles (Fig. 2D). No obvious anatomic or behavioral abnormalities, such as circling or head tossing, indicative of vestibular dysfunction, were apparent in homozygous mutant females or hemizygous mutant males, and the *Fgf16*-deficient animals were fertile, indicating that *Fgf16* does not have an obvious and unique role during mouse development. Since zebrafish *Fgf16* is expressed in the pectoral fin apical ectodermal ridge and *Fgf16* morpholino-treated (knockdown) zebrafish embryos have defects of pectoral fin (limb) bud outgrowth that are evident as early as 32 hrs post-fertilization (Nomura et al., 2006), our results show that limb/fin AER expression and function of *Fgf16* has diverged in the teleost and mammalian lineages.

The *Fgf16* otic expression pattern suggested possible roles in otic axis formation and/or cell fate decisions. To visualize the consequences of loss of *Fgf16* to inner ear morphogenesis, we filled $Fgf16^{IRESCreNeo}$ wild type or heterozygous control and homozygous or hemizygous mutant inner ear epithelia with latex paint at E15.5, a stage when the normal mouse ear has attained its mature morphology. At the gross anatomical level, a total of 12

mutant ears had a normal morphology and showed no obvious differences with wild type or heterozygous controls (Fig. 2E).

To test for cochlear sensory dysfunction, we measured auditory brainstem response (ABR) thresholds in each ear individually at approximately 6 weeks of age in animals of all three *Fgf16*$^{\text{IRES}CreNeo}$ genotypes. No significant differences in auditory thresholds were observed between wild type (n=3), heterozygous female (n=3) and hemizygous male mutant (n=7) animals, which showed thresholds averaging 29 dB, 28 dB and 29 dB, respectively.

Taken together, these results suggest that *Fgf16*-deficient inner ears are structurally and functionally normal. Thus, if *Fgf16* has a function in the ear, it must be redundant with other genes. The most closely related FGFs, which might be expected to share similar receptor specificity (FGFR3c>FGFR2c>FGFR1c, FGFR1b≫GFR4), are FGF9 and FGF20 (Zhang et al., 2006). *Fgf9* is expressed primarily in non-sensory regions of the otic epithelium, in the developing semicircular canal fusion plates and then canal ducts, and in Reissner's membrane in the cochlea. *Fgf9* is required directly for otic capsule morphogenesis and therefore indirectly for epithlelial morphogenesis (Pirvola et al., 2004). The finding that *Fgf16* is expressed adjacent to and possibly overlapping with some of the *Fgf9*-expressing vestibular tissues suggests the testable possibility that the *Fgf9* otic malformation phenotype could be exacerbated by loss of *Fgf16*. Redundancy between *Fgf16* and *Fgf20*, which is expressed between E13.5 and E15.5 in the developing sensory cells of the cochlear duct (Hayashi et al., 2008), but not at all in the vestibular system (O. Bermingham-McDonogh, pers. comm.) seems less likely. The other *Fgfs* expressed in the developing cristae include *Fgf3* and *Fgf10* (Wilkinson et al., 1989; Pirvola et al., 2000; Pauley et al., 2003, L. Urness and S. Mansour, unpublished). Both are required for normal morphogenesis of the semicircular canals (Mansour et al., 1993; Pauley et al., 2003; Ohuchi et al., 2005; Hatch et al., 2007) and it is possible that the additional loss of *Fgf16* might exacerbate their otic phenotypes, though the difference in receptor specificity (FGF3 and FGF10 signal primarily through FGFR2b) makes redundancy less likely.

The Fgf16 lineage is found in both sensory and non-sensory inner ear lineages

Fgf16^{IRESCreNeo} mice did not express CRE (data not shown), presumably due to the presence of the *Neo* cassette. To enable analysis of the *Fgf16* lineage, the *Neo* gene was removed by crossing *Fgf16*^{IRESCreNeo} mice to a FLPe deleter strain (Rodriguez et al., 2000). Mice harboring the *Neo*-deleted allele (*Fgf16*$^{IRESCre/Y}$, MGI accession number 3790784, symbolized *Fgf16*$^{tm1.1(Cre)Sms}$) were crossed to *Rosa26*$^{LacZ/LacZ}$ reporter mice (Soriano, 1999) for lineage studies. Embryos were collected at daily intervals between E9.5 and E15.5, and at P1, and stained with X-gal to detect β-galactosidase (βgal) activity in whole embryos (E9.5–14.5) or after dissection of the inner ears (E15.5, P1). βgal-positive (blue) cells were first apparent at E10.5, in the dorsolateral otic vesicle, although some cells in this region were reporter-negative (Fig. 3A,A′). The delay in the initial detection of βgal relative to the initiation of *Fgf16* mRNA expression at E9.0 is likely due to the additive effects of inefficient translation initiation at the IRES element, the time required for CRE protein synthesis and accumulation, LoxP excision, and finally, βgal synthesis and accumulation. Such delays have been noted for other *IRESCre* alleles (Ohyama and Groves, 2004; Vincent and Robertson, 2004; Lan et al., 2007). The patchiness of the expression could be caused by random inactivation of the *Fgf16*^{IRESCre} allele in heterozygous female embryos. At E11.5, βgal-positive cells were seen in the developing canal cristae and in scattered cells extending distally from the cristae at the margins of the vertical canal plate (vcp; Figs. 3B,B′). The same pattern of *Fgf16* lineage was seen at E12.5, after the canals started forming by fusion of the canal plates (Fig. 3C). βgal positive cells were found in the cristae and at the bases of the canal ducts extending distally (Figs. 3C,C_1,C_2), but not yet in the cochlear duct (Fig. 3C_3). At E13.5, βgal-positive cells were detected in all three cristae and in scattered cells

distributed throughout the non-sensory ducts of the anterior and posterior semicircular canals (a/psc), but these cells were more highly concentrated near the cristae (Fig. 3D,D_1). At E14.5, the pattern of βgal expression had not changed, but there were increasing numbers of positive cells in the semicircular canal ducts and expression in the cristae appeared to include cells throughout the thickness of the cristae, in precursors to both sensory and supporting cell lineages (Figs. 3E,E_1). *Fgf16* lineage was apparent in the lateral margin of the cochlear duct, particularly in the most apical regions (Figs. 3E,E_2). At E15.5 and P1, reporter-positive cells continued to be detected throughout the cristae, in both sensory and supporting domains, and in many cells of the anterior and posterior non-sensory semicircular canal ducts (Figs. 3F,F_1,G,G_1). Cochlear *Fgf16* lineage was maintained (Figs. 3F_2,G_2), and by P1, it was clear that these βgal positive cells were located at the base of the stria vascularis (Fig. 3G_2) and appeared to comprise the spiral prominence epithelium, the specific function of which is not understood in detail, but is likely to contribute to the maintenance of the endocochlear potential (Slepecky, 1996; Santi and Tsuprun, 2001).

Consistent with the in situ hybridization study, extra-otic sites of *Fgf16* lineage detected in our samples included the olfactory placode and epithelium, the endodermal pouch-derived parathyroid glands and some thymus cells, as well as the developing pituitary. We also noted *Fgf16* lineage in E14.5 limbs and lung, and P1 thyroid gland, which is derived from the dorsal oropharynx (foramen cecum, supplemental Fig. S2). We looked for *Fgf16* lineage in brown fat and heart, two sites of reported embryonic *Fgf16* expression (Miyake et al., 1998; Lavine et al., 2005). *Fgf16*-lineage was absent from brown fat (P1 and P15, data not shown), but could be detected in the sinoatrial node (the heart's pacemaker, supplemental Fig. S2). Further investigation will be required to correlate extra-otic *Fgf16* expression and lineage data and determine whether *Fgf16*-deficient mice have subtle or stress-activated phenotypes related to any of these lineages.

The vestibular cells marked by βgal activity from E11.5 and onwards corresponded precisely to the domains of *Fgf16* expression in the developing cristae marked by RNA in situ hybridization (Fig. 1G–R). Additional lineage-positive cells were located distally from the cristae in the non-sensory semicircular canal ducts, which did not themselves express significant levels of *Fgf16* mRNA until about E14.5 (Figs. 1O,O′), indicating that the *Fgf16*^{IRESCre} driver recapitulates endogenous ongoing *Fgf16* expression in the developing cristae, and in addition, between E11.5 and E14.5, marks duct cells that are likely derived from *Fgf16*-expressing cells in and/or immediately adjacent to the developing sensory patches. The cells adjacent to the developing cristae have been proposed as a "canal genesis zone" based on DiI fate-mapping of the developing chick canal pouch and the phenotypes of SU5402- or Noggin-treated chick ears (Chang et al., 1999; Gerlach et al., 2000; Chang et al., 2004) and of *Fgf10* and *Bmp4* mutant mouse ears, in which defective sensory patch development leads to semicircular canal agenesis (Pauley et al., 2003; Ohuchi et al., 2005; Chang et al., 2008). Our expression and *Fgf16* lineage tracing data strongly support the existence of a canal genesis zone in the mouse, as *Fgf16*-expressing cells apparently contribute to the semicircular canals as well as to the developing cristae. By E14.5, *Fgf16* expression was detected in the canals, so subsequent lineage observed in the canals may reflect a mixture of cristae- and canal-derived cells.

The cochlear expression of *Fgf16* mRNA at the lateral edges of the duct and the βgal-positive ROSA lineage corresponded precisely, except for a 2-day delay in detecting the lineage, suggesting that these *Fgf16*-expressing cells do not migrate or proliferate significantly.

Although our studies have not yet revealed a function for *Fgf16* in the inner ear, *Fgf16*^{IRESCre} mice could be used to inactivate floxed genes specifically in the developing

cristae and spiral prominence epithelial precursors. This might be useful in teasing apart the roles of cristae-expressed genes that are also expressed the other types of otic sensory epithelia. For example, *Bmp4* is expressed in developing cristae and at low levels in the maculae (Morsli et al., 1998; Chang et al., 2008), and *Fgf10* is expressed in all three types of sensory patches (Pirvola et al., 2000; Pauley et al., 2003), but whether the function of each gene is the same in each sensory patch is unknown. In addition, expression of $Fgf16^{IRESCre}$ in the progenitors of the spiral prominence epithelium provides an opportunity to probe gene function in that tissue. For example, Pendrin, encoded by *Slc26a4*, is expressed in the epithelial cells of both the stria vascularis and spiral prominence (Wangemann et al., 2004), but it is not known whether its role in endolymph homeostasis requires expression in both locations. Finally, by combining $Fgf16^{IRESCre}$ with a $Rosa26^{stopDTA}$ allele (Ivanova et al., 2005; Wu et al., 2006), it will be possible to ablate the *Fgf16* lineage and observe the consequences to inner ear development.

Methods

All work with mice complied with protocols approved by the University of Utah Institutional Animal Care and Use Committee. Embryo ages were determined by counting somite pairs or by considering noon on the day of vaginal plug detection to be E0.5.

RNA in situ hybridization

Fgf16 expression was analyzed at E8.5–10.5 by whole mount RNA in situ hybridization of CD-1 (Charles River Laboratories) embryos using a digoxigenin-labeled *Fgf16* RNA probe followed by cryosectioning as described previously (Miyake et al., 1998; Wright et al., 2003). For expression analysis at later stages, whole heads were fixed, embedded in paraffin, sectioned at 10 μm, and stained as described (Urness et al., 2008) using the same probe as for the whole mount expression analysis.

Generation and genotyping of the $Fgf16^{IRESCreNeo}$ and $Fgf16^{IRESCre}$ alleles

Recombination cloning (Zhang et al., 2002) was used to isolate from the λKO2 library (mouse strain129/Sv) a phage bearing a 9.3 kb fragment of *Fgf16* genomic DNA with a LoxP site inserted 4.8 kb downstream of exon 1 and flanked by a thymidine kinase gene. After recovery of the plasmid insert, an *IRES-Cre-PGKNeo* cassette (Arenkiel et al., 2003) was inserted into an artificial AscI site generated in the first exon of *Fgf16* and disrupting the 63rd odon. The resulting targeting vector was linearized and electroporated into R1–45 ES cells, which were selected in G-418 and ganciclovir as described (Li et al., 2007). Since *Fgf16* is located on the X chromosome, random insertions of the targeting vector were expected to retain a LoxP site, whereas correctly targeted cell lines were expected to lack the LoxP site, which was located near one end of the targeting vector. The presence or absence of the LoxP site was determined by PCR amplification using *Fgf16* primers 501 (5′-CCCACTGTTCTTGCCTCTTC-3′) and 502 (5′-GGTTTTGGTGCTGGAGATTG-3′), which flank the LoxP site, and yielded a 376 bp wild type or a 450 bp LoxP-containing DNA fragment. ES clones lacking a LoxP site were analyzed by Southern blot hybridization of *Tth111I*-digested DNA using a 5′ flanking external probe and of *HindIII*-digested DNA using a 3′ internal probe was used to confirm correct targeting (Figs. 2A,B). Of 192 drug resistant cell lines, 5 were correctly targeted. Following injection into C57Bl/6 blastocysts, several correctly targeted cell lines generated highly chimeric males that transmitted the targeted allele to offspring. The $Fgf16^{IRESCreNeo}$ allele is officially symbolized as $Fgf16^{tm1(Cre)Sms}$, MGI accession number 3790778. In subsequent crosses, the wild type and mutant alleles were distinguished by PCR analysis using a three-primer mix containing primers 73 (Neo reverse-5′-TTCAGTGACAACGTCGAGCAC-3′), 418 (*Fgf16* exon 1 forward-5′-GTCTTTGCCTCCTTGGACTG-3′) and 419 (*Fgf16* exon 1 reverse-5′-

CCGTTGGGGAAGATCTCAAG -3′), which produced a wild type band of 218 bp and a mutant band of 691 bp.

To remove the *Neo* cassette, chimeric males capable of transmitting $Fgf16^{IRESCreNeo}$ were mated to *FLP*-expressing mice (Rodriguez et al., 2000) and the progeny were screened for loss of the *PGK-Neo* selection cassette by PCR. Primers 418 and 419 as above and 557 (*Cre* forward-5′-CAATACCGGAGATCATGCAAG-3′) produced a wild type band of 218 bp and a mutant band of 360 bp. The *Neo* deleted allele is officially symbolized as $Fgf16^{tm1.1(Cre)Sms}$, MGI accession number 3790784.

RT-PCR analysis

Total RNA was isolated from female wild type, female heterozygous and male hemizygous mutant embryos at E9.0. Following reverse transcription with an oligo(dT) primer, cDNA fragments were PCR-amplified using *Fgf16*-specific primers 418 (exon 1, forward) and 569 (exon 2, reverse-5′-GCCAAGCTGATAAATTCCAGA-3′). A 351 bp region within the *Hprt* positive control gene was PCR-amplified using primers 33 (5′-CCTGCTGGATTACATTAAAGCACTG-3′) and 34 (5′-GTCAAGGGCATATCCAACAACAAAC-3′).

Paint-filling and auditory brainstem response (ABR) threshold measurements

E15.5 embryos were fixed in Modified Carnoy's solution, cleared in methyl salicylate and the ears were filled through the saccule with white latex paint as described (Morsli et al., 1998). For ABR studies, 3–5 week old mice were anesthetized using 0.02 ml/g Avertin. Thresholds for click stimuli (47 μsec duration, 29.3/sec) presented to each ear individually were determined using high frequency transducers controlled and analyzed by SmartEP software (Intelligent Hearing Systems) (Zheng et al., 1999).

Fgf16 lineage analysis

We crossed $Rosa26^{LacZ/LacZ}$ reporter females (Soriano, 1999) to $Fgf16^{IRESCre/Y}$ males or heterozygous or homozygous $Fgf16^{IRESCre}$ females to homozygous reporter males. Embryos or dissected ears harboring both the $Rosa26^{LacZ}$ and $Fgf16^{IRESCre}$ alleles were stained with X-gal and sectioned as described (Yang et al., 1997).

Supplementary Material

Refer to Web version on PubMed Central for supplementary material.

Acknowledgments

We thank Steve Elledge for the recombination screening system reagents, Ben Arenkiel and Mario Capecchi for the IRESCreNeo cassette, and Susan Tamowski of the University of Utah Transgenic/Gene Targeting Facility for chimera generation. We are grateful to Chaoying Li for completing the lineage staining, to Dr. Steven Bleyl for heart expertise, and to Dr. Gary Schoenwolf for developmental expertise and constructive criticism of the manuscript. Supported by NIH grants R01-DC04185 (SLM, LDU and EH) and T32-GM007464 (EH).

References

Arenkiel BR, Gaufo GO, Capecchi MR. Hoxb1 neural crest preferentially form glia of the PNS. Dev Dyn. 2003; 227:379–386. [PubMed: 12815623]

Bok J, Chang W, Wu DK. Patterning and morphogenesis of the vertebrate inner ear. Int J Dev Biol. 2007; 51:521–533. [PubMed: 17891714]

Brigande JV, Iten LE, Fekete DM. A fate map of chick otic cup closure reveals lineage boundaries in the dorsal otocyst. Dev Biol. 2000; 227:256–270. [PubMed: 11071753]

Chang W, Brigande JV, Fekete DM, Wu DK. The development of semicircular canals in the inner ear: role of FGFs in sensory cristae. Development. 2004; 131:4201–4211. [PubMed: 15280215]

Chang W, Lin Z, Kulessa H, Hebert J, Hogan BL, Wu DK. Bmp4 is essential for the formation of the vestibular apparatus that detects angular head movements. PLoS Genet. 2008; 4:e1000050. [PubMed: 18404215]

Chang W, Nunes FD, De Jesus-Escobar JM, Harland R, Wu DK. Ectopic noggin blocks sensory and nonsensory organ morphogenesis in the chicken inner ear. Dev Biol. 1999; 216:369–381. [PubMed: 10588886]

Chapman SC, Cai Q, Bleyl SB, Schoenwolf GC. Restricted expression of Fgf16 within the developing chick inner ear. Dev Dyn. 2006; 235:2276–2281. [PubMed: 16786592]

Gerlach LM, Hutson MR, Germiller JA, Nguyen-Luu D, Victor JC, Barald KF. Addition of the BMP4 antagonist, noggin, disrupts avian inner ear development. Development. 2000; 127:45–54. [PubMed: 10654599]

Hatch EP, Noyes CA, Wang X, Wright TJ, Mansour SL. Fgf3 is required for dorsal patterning and morphogenesis of the inner ear epithelium. Development. 2007

Hayashi T, Ray CA, Bermingham-McDonogh O. Fgf20 is required for sensory epithelial specification in the developing cochlea. J Neurosci. 2008; 28:5991–5999. [PubMed: 18524904]

Ivanova A, Signore M, Caro N, Greene ND, Copp AJ, Martinez-Barbera JP. In vivo genetic ablation by Cre-mediated expression of diphtheria toxin fragment A. Genesis. 2005; 43:129–135. [PubMed: 16267821]

Kiernan, AE.; Steel, KP.; Fekete, DM. Development of the mouse inner ear. In: Rossant, J.; Tam, PPL., editors. Mouse development: Patterning, morphogenesis and organogenesis. London: Academic Press Inc; 2002. p. 539-566.

Lan Y, Wang Q, Ovitt CE, Jiang R. A unique mouse strain expressing Cre recombinase for tissue-specific analysis of gene function in palate and kidney development. Genesis. 2007; 45:618–624. [PubMed: 17941042]

Lavine KJ, Yu K, White AC, Zhang X, Smith C, Partanen J, Ornitz DM. Endocardial and epicardial derived FGF signals regulate myocardial proliferation and differentiation in vivo. Dev Cell. 2005; 8:85–95. [PubMed: 15621532]

Li C, Scott DA, Hatch E, Tian X, Mansour SL. Dusp6 (Mkp3) is a negative feedback regulator of FGF-stimulated ERK signaling during mouse development. Development. 2007; 134:167–176. [PubMed: 17164422]

Mansour SL, Goddard JM, Capecchi MR. Mice homozygous for a targeted disruption of the proto-oncogene int-2 have developmental defects in the tail and inner ear. Development. 1993; 117:13–28. [PubMed: 8223243]

Miyake A, Konishi M, Martin FH, Hernday NA, Ozaki K, Yamamoto S, Mikami T, Arakawa T, Itoh N. Structure and expression of a novel member, FGF-16, on the fibroblast growth factor family. Biochem Biophys Res Commun. 1998; 243:148–152. [PubMed: 9473496]

Morsli H, Choo D, Ryan A, Johnson R, Wu DK. Development of the mouse inner ear and origin of its sensory organs. J Neurosci. 1998; 18:3327–3335. [PubMed: 9547240]

Nomura R, Kamei E, Hotta Y, Konishi M, Miyake A, Itoh N. Fgf16 is essential for pectoral fin bud formation in zebrafish. Biochem Biophys Res Commun. 2006; 347:340–346. [PubMed: 16815307]

Ohuchi H, Yasue A, Ono K, Sasaoka S, Tomonari S, Takagi A, Itakura M, Moriyama K, Noji S, Nohno T. Identification of cis-element regulating expression of the mouse Fgf10 gene during inner ear development. Dev Dyn. 2005; 233:177–187. [PubMed: 15765517]

Ohyama T, Groves AK. Generation of Pax2-Cre mice by modification of a Pax2 bacterial artificial chromosome. Genesis. 2004; 38:195–199. [PubMed: 15083520]

Pauley S, Wright TJ, Pirvola U, Ornitz D, Beisel K, Fritzsch B. Expression and function of FGF10 in mammalian inner ear development. Dev Dyn. 2003; 227:203–215. [PubMed: 12761848]

Pirvola U, Spencer-Dene B, Xing-Qun L, Kettunen P, Thesleff I, Fritzsch B, Dickson C, Ylikoski J. FGF/FGFR-2(IIIb) signaling is essential for inner ear morphogenesis. J Neurosci. 2000; 20:6125–6134. [PubMed: 10934262]

Pirvola U, Zhang X, Mantela J, Ornitz DM, Ylikoski J. Fgf9 signaling regulates inner ear morphogenesis through epithelial-mesenchymal interactions. Dev Biol. 2004; 273:350–360. [PubMed: 15328018]

Rodriguez CI, Buchholz F, Galloway J, Sequerra R, Kasper J, Ayala R, Stewart AF, Dymecki SM. High-efficiency deleter mice show that FLPe is an alternative to Cre-loxP. Nat Genet. 2000; 25:139–140. [PubMed: 10835623]

Santi, PA.; Tsuprun, VL. Physiology of the Ear. Singular; 2001. Cochlear Microanatomy and Ultrastructure. p look this up

Slepecky, NB. Cochlear Structure. In: Dallos, P.; Popper, AN.; Fay, RR., editors. The Cochlea. New York: Springer-Verlag; 1996. p look this up

Soriano P. Generalized lacZ expression with the ROSA26 Cre reporter strain. Nat Genet. 1999; 21:70–71. [PubMed: 9916792]

Streit A. Extensive cell movements accompany formation of the otic placode. Dev Biol. 2002; 249:237–254. [PubMed: 12221004]

Swanson GJ, Howard M, Lewis J. Epithelial autonomy in the development of the inner ear of a bird embryo. Dev Biol. 1990; 137:243–257. [PubMed: 2303163]

Urness LD, Li C, Wang X, Mansour SL. Expression of ERK signaling inhibitors Dusp6, Dusp7, and Dusp9 during mouse ear development. Dev Dyn. 2008; 237:163–169. [PubMed: 18058922]

Vincent SD, Robertson EJ. Targeted insertion of an IRES Cre into the Hnf4alpha locus: Cre-mediated recombination in the liver, kidney, and gut epithelium. Genesis. 2004; 39:206–211. [PubMed: 15282747]

Wangemann P, Itza EM, Albrecht B, Wu T, Jabba SV, Maganti RJ, Lee JH, Everett LA, Wall SM, Royaux IE, Green ED, Marcus DC. Loss of KCNJ10 protein expression abolishes endocochlear potential and causes deafness in Pendred syndrome mouse model. BMC Med. 2004; 2:30. [PubMed: 15320950]

Wilkinson DG, Bhatt S, McMahon AP. Expression pattern of the FGF-related proto-oncogene int-2 suggests multiple roles in fetal development. Development. 1989; 105:131–136. [PubMed: 2680421]

Wright TJ, Hatch EP, Karabagli H, Karabagli P, Schoenwolf GC, Mansour SL. Expression of mouse fibroblast growth factor and fibroblast growth factor receptor genes during early inner ear development. Dev Dyn. 2003; 228:267–272. [PubMed: 14517998]

Wu DK, Nunes FD, Choo D. Axial specification for sensory organs versus non-sensory structures of the chicken inner ear. Development. 1998; 125:11–20. [PubMed: 9389659]

Wu S, Wu Y, Capecchi MR. Motoneurons and oligodendrocytes are sequentially generated from neural stem cells but do not appear to share common lineage-restricted progenitors in vivo. Development. 2006; 133:581–590. [PubMed: 16407399]

Yang W, Musci TS, Mansour SL. Trapping genes expressed in the developing mouse inner ear. Hear Res. 1997; 114:53–61. [PubMed: 9447918]

Zhang P, Li MZ, Elledge SJ. Towards genetic genome projects: genomic library screening and gene-targeting vector construction in a single step. Nat Genet. 2002; 30:31–39. [PubMed: 11753384]

Zhang X, Ibrahimi OA, Olsen SK, Umemori H, Mohammadi M, Ornitz DM. Receptor specificity of the fibroblast growth factor family. The complete mammalian FGF family. J Biol Chem. 2006; 281:15694–15700. [PubMed: 16597617]

Zheng QY, Johnson KR, Erway LC. Assessment of hearing in 80 inbred strains of mice by ABR threshold analyses. Hear Res. 1999; 130:94–107. [PubMed: 10320101]

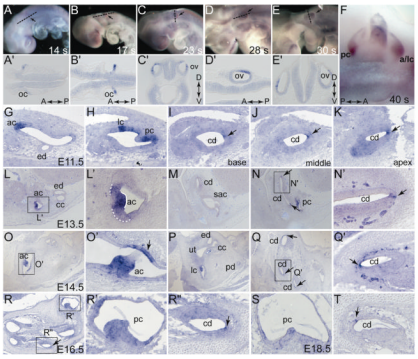

Figure 1. *Fgf16* mRNA expression from E9.0–E18.5

Whole-mount 14-somite (A), 17-somite (B), 23-somite (C), and 28-somite (D), 30-somite (E), and 40-somite (F) embryos were probed with labeled antisense *Fgf16* cRNA. Anterior is to left (A,B,C,D,E) or right (F). White lines indicate the plane of coronal (A′,B′,D′) or transverse (D′,E′) sections shown in panels below the whole mounts, black arrows indicate the otic vesicle. *Fgf16* expression in transverse (G-R″) or sagittal (S,T) paraffin sections. (L ′) Solid white line indicates strong expression in anterior crista, dotted white line indicates weaker expression in cells adjacent to the crista. Abbreviations: A, anterior; ac, anterior crista; a/lc, anterior and lateral criate; cc, common crus; cd, cochlear duct; D, dorsal; ed, endolymphatic duct; lc, lateral crista; oc, otic cup; ov, otic vesicle; P, posterior: pc, posterior crista; sac, saccule; ut, utricle; V, ventral.

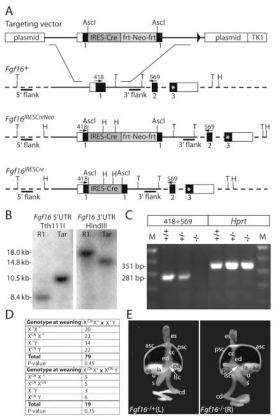

Figure 2. Gene targeting at the *Fgf16* locus

(A) Structure of the linearized *Fgf16* targeting vector and depiction of the wild type *Fgf16* allele (*Fgf16*+), the correctly targeted mutant allele in ES cells and offspring of chimeric mice ($Fgf16^{IRESCreNeo}$) and the targeted allele after exposure to FLP recombinase ($Fgf16^{IRESCre}$). Mouse genomic *Fgf16* DNA is depicted with solid lines; dotted lines indicate *Fgf16* genomic DNA that is not present in the targeting vector; untranslated regions are shown as open boxes, protein coding regions as solid boxes. The *IRES-Cre* cassette is shown as a dark grey box; the *Neo* cassette flanked by frt sites as a light grey box; the stop codon in the *Fgf16* frame in exon 3 as an asterisk. The plasmid backbone and the thymidine kinase (TK1) gene are depicted as open boxes. Recognition sites for *Tth111I* and *HindIII*, used in Southern analysis are indicated by "T" and "H" respectively. Probes used for Southern analysis are shown as black bars. Numbered arrows indicate the identity, position and directionality of primers used for the RT-PCR assay. (B) Southern blot hybridization assay demonstrating correct targeting of *Fgf16* in ES cells. *Tth111I*-digested genomic DNA from either the R1–45 ES cell line (R1) or a correctly targeted cell line (Tar) probed with the external 5′ probe. (C) RT-PCR assay used to detect *Fgf16* mRNA in wild type and mutant animals. Total E9.0 RNA isolated from female wild type (+/+), female heterozygous (+/−) and male hemizygous mutant (−/Y) embryos was PCR-amplified using primers 418 and 569. A 351 bp *Hprt* cDNA fragment was amplified from all samples as a positive control. (D) *Fgf16* backcross and intercross genotypes. Offspring of the indicated crosses were genotyped at weaning. P-values were determined using the method of χ^2. The $Fgf16^{IRESCreNeo}$ allele is defined as X^{Neo}. (E) *Fgf16*-deficient inner ears were morphologically normal. Representative lateral views of paint-filled inner ears from E15.5 female heterozygous control and $Fgf16^{IRESCreNeo}$ homozygous mutants. Labeled structures: aa, anterior ampulla; asc, anterior semicircular canal; cc, common crus; cd, cochlear duct; ed, endolymphatic duct; es, endolymphatic sac; la, lateral ampulla; lsc, lateral semicircular canal; pa, posterior ampulla; psc, posterior semicircular canal; s, saccule; u, utricle.

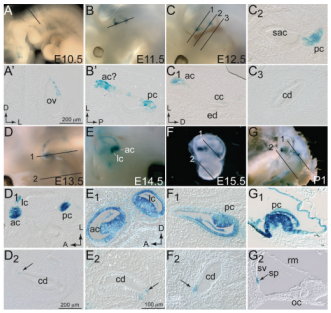

Figure 3. Lineage of *Fgf16*-expressing cells at E10.5-P1

Embryos (A–D), inner ears (E,F) or heads (G) harboring both the *Rosa26*^{LacZ} reporter and *Fgf16*^{CreNeo} alleles were stained with X-gal at E10.5 (A), E11.5 (B), E12.5 (C), E13.5 (D), E14.5, (E) E15.5 (F), and P1 (G). Anterior is to left in all whole mount panels except E, in which anterior is to the right. Black lines (numbered as appropriate) indicate the plane of transverse (A,C,F,G), coronal (B,D) sections shown in panels below the whole mounts. Sagittal sections of E14.5 left ear (E) were taken in the plane of view, with E_1 more lateral than E_2. Scale bar in A′ and D_1 applies to B′-D_2. Scale bar in E_1 applies to E_2–G_2 Abbreviations: ac, anterior crista; cd, cochlear duct; ed, endolymphatic duct; lc, lateral crista; oc, organ of Corti; ov, otic vesicle; pc, posterior crista; rm; Reissner's membrane; sac, saccule; sp, spiral prominence; sv, stria vascularis.